ELSEVIER

Thermochimica Acta 282/283 (1996) 411–423

thermochimica acta

Crystal structure and mechanical properties of ODPA–DMB polyimide fibers[1]

Young Ho Kim[2], Frank W. Harris, Stephen Z.D. Cheng *

Maurice Morton Institute and Department of Polymer Science, The University of Akron, Akron, Ohio, 44325-3909, USA

Abstract

A new polyimide has been synthesized from 4,4′-oxydiphthalic anhydride (ODPA) and 2,2′-dimethyl-4,4′-diaminobiphenyl (DMB) via a one-step polycondensation reaction. This polyimide can be dissolved in polar organic solvents and spun into fiber form using a dry-jet wet-spinning method. The crystal unit cell of highly drawn and annealed ODPA–DMB fibers has been determined to be triclinic with $a = 1.05$ nm, $b = 0.871$ nm, $c = 2.14$ nm, $\alpha = 45.6°$, $\beta = 53.7°$ and $\gamma = 61.4°$. It has been found that crystallinity and orientation are critically dependent upon draw ratio. Furthermore, the overall orientation and crystal orientation developed in the ODPA–DMB fibers exhibit different behavior. In the high draw ratio region (a draw ratio of above 3), the degree of crystal orientation levels off to reach a constant while the overall orientation develops continuously. Tensile properties of the fibers in this region also show significant improvement. This indicates that the enhancement of the tensile properties must be associated with molecular orientation in the non-crystalline region of the fibers. The pre-existing structure developed during the fiber spinning also drastically affects subsequent drawing and annealing processes and ultimate tensile properties due to the competition between molecular orientation and crystallization.

Keywords: ODPA; DMB; Polyimide fiber; Drawing; Crystal unit cell; Triclinic; Orientation; Crystal orientation; Crystallinity; Tensile properties

* Corresponding author.

[1] Dedicated to Takeo Ozawa on the Occasion of his 65th Birthday.

[2] Permanent address: Department of Textile Engineering, College of Engineering, Soong-Sil University, Seoul, 156-743, Korea.

SSDI 0040-6031(96)02805-5

1. Introduction

In several recent publications, we have reported a new series of aromatic polyimide fibers developed in our laboratories [1–5]. These polyimides were synthesized via a one-step polycondensation reaction in phenolic solvents at elevated temperatures, and poly(amic acid) precursors were thus not isolated. This requires a specific molecular design to construct the polyimides, which keep the chain linearity and rigidity while remaining soluble in these solvents [6, 7]. Obtaining high molecular weight materials and controlling the crystallization rate are two essential factors to achieve good mechanical properties. The molecular weight is directly associated with fiber spinnability and structure-defect density in the fibers. Furthermore, during the fiber spinning, drawing and annealing, it is ideally desirable to achieve a maximum degree of orientation, followed by crystallization. Note that the crystallization during the formation of fibers critically affects the ultimate fiber tensile properties.

This series of aromatic polyimide fibers developed in our laboratory was spun via a dry-jet wet-spinning method [8]; they show excellent mechanical properties, combined with high thermal and thermo-oxidative stability. They have been potential candidates in high-temperature structure composite applications. A common feature of these polyimide fibers is that all of them are based on 3,3′,4,4′-biphenyltetracarboxylic dianhydride and different modified diamines [1–5]. The solubility of these polyimides is limited to a few polar solvents such as *m*-cresol and *p*-chlorophenol, which hampers practical applications in industry. Our attempt is to investigate the effect of different dianhydrides on the polyimide fiber processing, structure and properties. This publication reports the first result along this research line for the fibers spun from a new aromatic polyimide synthesized from 4,4′-oxydiphthalic anhydride (ODPA) and 2,2′-dimethyl-4,4′-diaminobiphenyl (DMB). The chemical structure of ODPA–DMB polyimide is

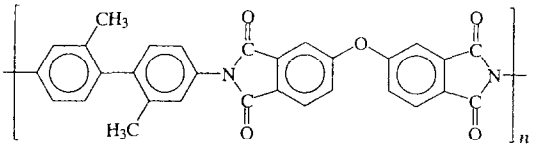

2. Experimental section

2.1. Materials and sample preparations

The method to obtain ODPA–DMB polyimide was described in a previous paper [9]. One-step polymerization was used for carrying out the synthesis in *m*-cresol and poly(amic acid)s were thus not isolated. The ODPA–DMB polyimide powder was dissolved in phenol with the concentration of 15% (w/w) at 50°C. The solution was degassed completely before spinning. Fiber was spun with a dry-jet spinning method. Since the solidification temperature of phenol is 41°C, the temperature of polymer

solution should be higher than this temperature. The spinning solution was heated to 65°C and extruded from a 0.25 mm diameter spinneret. The filament passed through a dry-gap of about 10 cm into a methanol coagulation bath with a bath length of 1 m. As-spun fibers were wound onto a take-up roller that was adjusted to the proper speed with respect to the spinning speed at the spinneret. The roller containing the as-spun fibers was left in the fresh methanol bath for 2 days. The methanol was changed several times in order to achieve complete precipitation. The as-spun fibers were dried in a vacuum oven at 250°C for 2 days, and finally dried at 300°C for 1 h under vacuum. Fibers with different draw ratios were prepared by a continuous zone-drawing method through the control of the take-up roller and feed roller speeds. A 6.0 mm diameter hot pin was used in direct contact with the fiber as the zone oven and the temperature was controlled at 400°C.

2.2. *Instrument and experiments*

Overall orientation in the drawn fibers was determined by the optical birefringence method. A Leitz Laborlux 12POLS(Leica) having a 30-order tilting compensator was coupled with an Olympus polarized light microscope (PLM) and used to measure the optical retardation of the fibers. The birefringence, Δn, was calculated from the measured retardation and fiber thickness following the standard procedure [10].

Wide-angle X-ray diffraction (WAXD) experiments were carried out with a 12-kW Rigaku rotating anode X-ray generator. The as-spun, drawn and annealed ODPA–DMB fiber patterns were recorded on flat-film in a vacuum camera. Silicone powder (325 mesh) was used to calculate the exact distance between the sample and flat-film using its reflection peak at $2\theta = 28.44°$. The crystal unit cell dimension and type of lattice were determined using the method of reciprocal lattice. The wavelength (λ) of the Cu K_α X-ray incident beam was 0.154 nm. Diffraction patterns of the fibers with different draw ratios were also taken from a Siemens two-dimensional detector with an exposure time of 2 h followed by subtraction of air scattering. WAXD powder patterns of the drawn fibers were obtained by integration of all the intensities along the azimuthal direction with respect to the 2θ direction. X-ray crystallinity was determined using this powder pattern by comparing the total area and amorphous area between $2\theta = 5°$ and 45°. The density of the as-spun and drawn fibers was measured on a density gradient column using hexane–carbon tetrachloride mixed solvent system at 25°C.

Crystal orientations were determined using the Siemens 2-D detector fiber pattern through an azimuthal integration of the intensity of the (110) plane ($2\theta = 16.6° \sim 17.2°$). The orientation factor was calculated from the Hermans equation

$$f_c(110) = \frac{3\langle \cos^2 \Phi_c \rangle - 1}{2} \tag{1}$$

where f_c is the orientation factor along the fiber direction, and Φ_c represents the angle between the fiber direction and the 110 reflection of the crystal unit cell. The numerical values of the mean-square cosines in Eq. (1) can be determined from the corrected intensity distribution diffracted from the meridian crystallographic plane, $I_c(\Phi_c, \alpha)$,

averaged over the entire surface of the orientation sphere

$$\langle \cos^2 \phi_c \rangle = \frac{\int_0^{\pi/2} \int_0^{2\pi} I_c(\phi_c, \alpha) \cos^2 \phi_c \sin \phi_c \, d\alpha d\phi_c}{\int_0^{\pi/2} \int_0^{2\pi} I_c(\phi_c, \alpha) \sin \phi_c \, d\alpha d\phi_c} \tag{2}$$

Mechanical measurements of the fibers were also conducted on the Rheometrics Solids Analyzer (Model RSA II). Single filaments with different draw ratios were clamped into a sample holder. The stress–strain curves were obtained using tension mode at 25°C with a strain rate of 0.002 s^{-1}. The sample fiber length was 2.3 cm. The tensile modulus was obtained from the initial slope of the stress–strain curve. Tensile strength and strain at break were read directly from the curve. Each data point was averaged based on at least 20 time measurements.

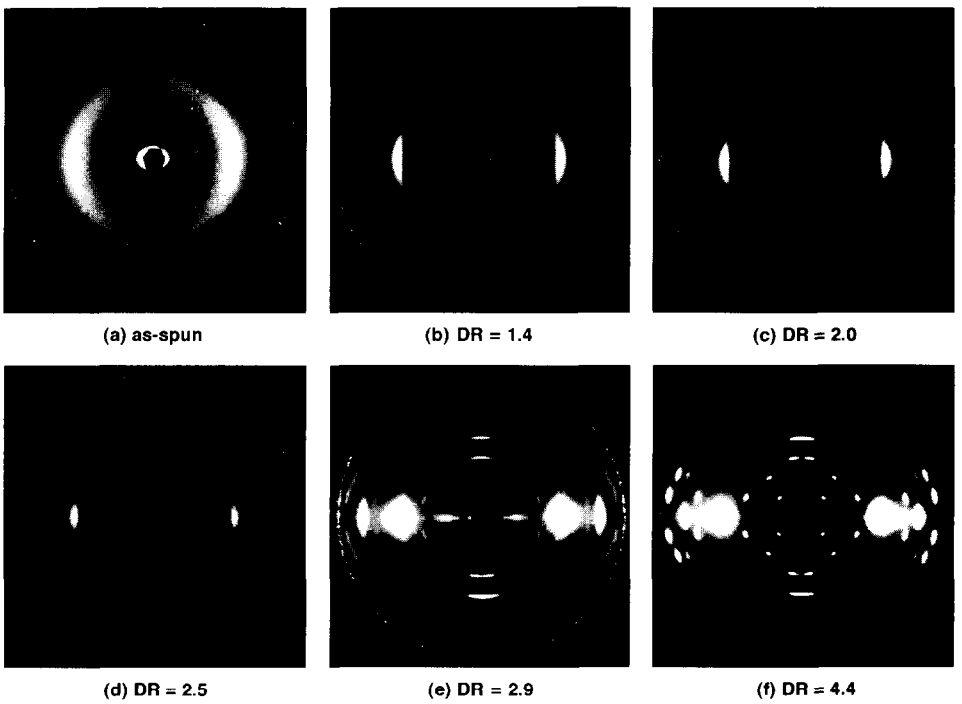

Fig. 1. Set of WAXD fiber patterns at different draw ratios: (a) as-spun fibers, (b) draw ratio = 1.4, (c) draw ratio = 2.0, (d) draw ratio = 2.5, (e) draw ratio = 2.9, (f) draw ratio = 4.4.

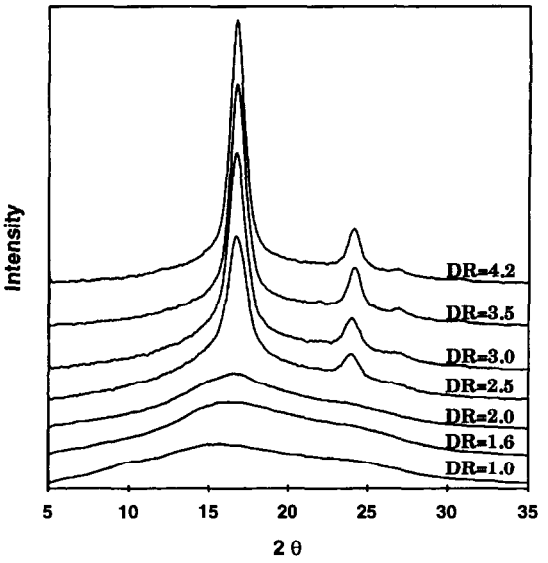

Fig. 2. Set of WAXD fiber patterns scanning along the equatorial direction at different draw ratios.

3. Results and Discussion

3.1. Unit cell determination

Fig. 1 shows WAXD patterns of ODPA–DMB fibers at different draw ratios and Fig. 2 shows the WAXD curves of ODPA–DMB fibers along the equatorial direction at different draw ratios. It is clear that as the draw ratio increases, the reflection spots become narrowed and crystallinity increases. This indicates that ODPA–DMB is crystallizable and crystal structure develops with increasing draw ratio and annealing time. Consider the WAXD fiber pattern having a draw ratio 4.4 (Fig. 1f). No reflection spots along the meridian can be found in the WAXD fiber pattern, but rather the pattern shows an "X" shape of the reflections about the meridian (fiber) direction, which may be indicative of a triclinic lattice system. To determine the crystal unit cell, a conversion of reflection spots in Cartesian coordinates (X and Y) to reciprocal coordinates (X^* and Y^*) in a reciprocal crystal lattice is necessary through the relationships of

$$X^* = [2 - Y^{*2} - 2(1 - Y^{*2})^{1/2}\cos(2\theta)]^{1/2} \text{ and } Y^* = \frac{Y}{(Y^2 + R^2)^{1/2}} \quad (3)$$

where R is the distance between the sample and X-ray films, Y is the height of the reflection spot from its equatorial line, and 2θ is the diffraction angle. For a triclinic

lattice, the Y^* values further indicate the distances between different layers. One starts by finding an hk0 reciprocal lattice net which is a parallelogram with edges of the a^* and b^* that account for the values determined from the equatorial reflections. In this case, $Y=0$, thus $Y_0^*=0$, and $X_0^*=[2-2\cos 2\theta]^{1/2}$. The smallest distance between the center of the X-ray incident beam and the reflection spot corresponds to the lowest index. In trying to index the quadrant diffraction spots, one calculates the Y^* values of the reflection spots on different layers. The distances obtained from the different layers lead to a least common multiple which usually corresponds to the value of the c-axis in the unit cell. Computer refinement is then conducted to achieve the fit with the least error between experimental results and calculated data based on a continuous refinement program starting with the unit cell shape and size obtained from manual calculations [3]. For OPDA–DMB, a total of twenty spots are observed within the silicone ring pattern ($2\theta < 28.44°$). Two spots are on the equator, twelve spots are on the first, second, and third layers with four spots each and the 4th, 5th and 6th layers possess two spots on each layer. They have been used to determine the unit cell parameters. The crystal unit cell of the highly drawn ODPA–DMB fibers was determined to be triclinic with $a=1.05$ nm, $b=0.871$ nm, $c=2.14$ nm, $\alpha=45.6°$, $\beta=53.7°$, and $\gamma=61.4°$. The length of the c-axis in the ODPA–DMB crystal unit cell is almost the same as the molecular repeating unit length. A detailed list of observed 2θ

Table 1
Crystallographic parameters of highly drawn ODPA–DMB fibers

	2θ deg		d-spacing (nm)		
Miller indices	Calc.	Expt.	Calc.	Expt.	Intensity[a]
110	16.82	16.93	0.527	0.524	vs
210	24.23	24.26	0.367	0.367	s
001	6.33	6.33	1.395	1.397	s
111	12.67	12.68	0.698	0.698	s
$\bar{1}\bar{1}1$	22.09	22.09	0.402	0.403	m
$2\bar{1}1$	27.66	27.29	0.323	0.327	s
112	10.94	10.91	0.809	0.811	s
002	12.69	12.65	0.698	0.699	w
$1\bar{1}2$	24.94	24.86	0.357	0.358	m
312	27.02	26.47	0.330	0.337	s
113	12.63	12.65	0.701	0.700	s
003	19.08	19.11	0.465	0.464	w
203	21.93	22.14	0.405	0.402	w
$\bar{1}13$	23.69	23.96	0.376	0.372	m
114	16.75	16.78	0.529	0.528	s
024	24.82	24.67	0.359	0.361	m
115	22.00	22.03	0.404	0.404	m
225	22.87	22.84	0.389	0.389	w
226	25.41	25.53	0.351	0.349	m
116	27.81	27.82	0.321	0.321	w

[a] The intensities were measured semiquantitatively: very strong (vs), strong (s), medium (m) and weak (w).

Table 2
Crystal unit cell parameters for ODPA-based polyimides

Polyimides	Crystal lattice	Unit cell parameters (*c-axis)	Repeating units	Crystal density/ (g cm^{-3})
ODPA–DMB	Triclinic	1.05, 0.871, 2.14* 45.6°, 53.7°, 61.4°	2	1.44
ODPA–P[a]	Orthorhombic	0.85, 1.08, 4.30*	8	1.62
ODPA–PP[b]	Orthorhombic	0.85, 1.09, 4.36*	8	1.52
ODPA POP[c]	Monoclinic	0.52, 1.08, 3.82* $\gamma = 105°$	4	1.52
ODPA–$(PO)_2$P[d]	Triclinic	0.94, 1.05, 2.61* 90°, 95°, 98°	4	1.47

[a] Polyimide synthesized from ODPA and *p*-phenylene diamine.
[b] Polyimide synthesized from ODPA and 4,4′-diamino biphenyl.
[c] Polyimide synthesized from ODPA and 4,4′-oxydianiline.
[d] Polyimide synthesized from ODPA and 1,4-bis (4-aminophenoxy) benzene.

angles, *d*-spacings, as well as their corresponding intensities for these twenty reflection spots observed is given in Table 1. The calculated data are also included in this table based on the refined unit cell parameters. A crystallographic volume of 1.1204 nm^3 can thus be calculated. Assuming two monomeric repeating units in each unit cell, a crystallographic density (100% crystallinity) of 1.442 g cm^{-3} is determined from the molar mass of the repeating unit (486.5 g mol^{-1}).

It is also interesting to compare the unit cell of ODPA–DMB with other ODPA-based polyimides as listed in Table 2 [5, 11]. Most crystal lattices for these polyimides are orthorhombic or monoclinic and contain 4 or 8 repeating units in one unit cell. Almost without exception, the *c*-axis dimensions of these polyimide crystals are double the chemical repeating unit length. However, for ODPA–DMB crystals, there are only two repeating units in the unit cell and the length of the *c*-axis is the same as the repeating unit length. The triclinic lattice found in this fiber may be associated with the diamine used in ODPA–DMB. It has also been found that most of the polyimides containing DMB and 3,3′-dimethyl-4,4′-diaminobiphenyl (OTOL) possess a triclinic lattice [4, 5, 11, 12].

3.2. *Crystallinity and orientation*

Fig. 3 shows the density change of ODPA–DMB fibers with different draw ratios. As the draw ratio initially increases, the density increases almost linearly until a draw ratio of three where the increase gradually levels off. The density of as-spun fibers is around 1.300 g cm^{-3} and that of highly drawn fibers with a draw ratio of 4.4 reaches 1.347 g cm^{-3}. Fig. 4 illustrates the relationship between the degree of crystallinity obtained from WAXD experiments and the density of ODPA–DMB fibers. The fibers show

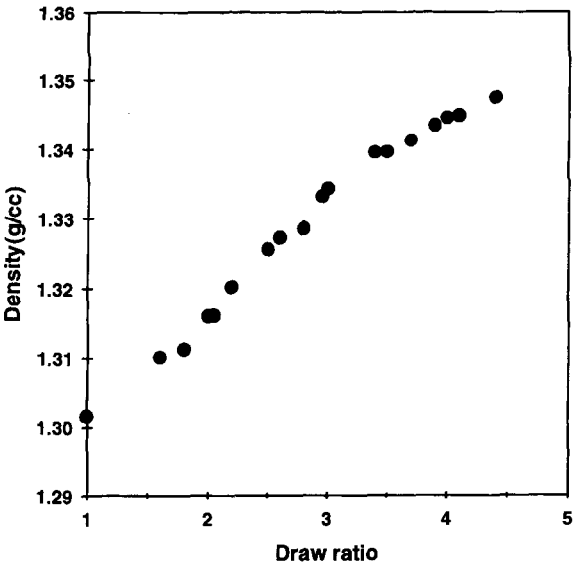

Fig. 3. Relationship between densities of ODPA–DMB and draw ratio.

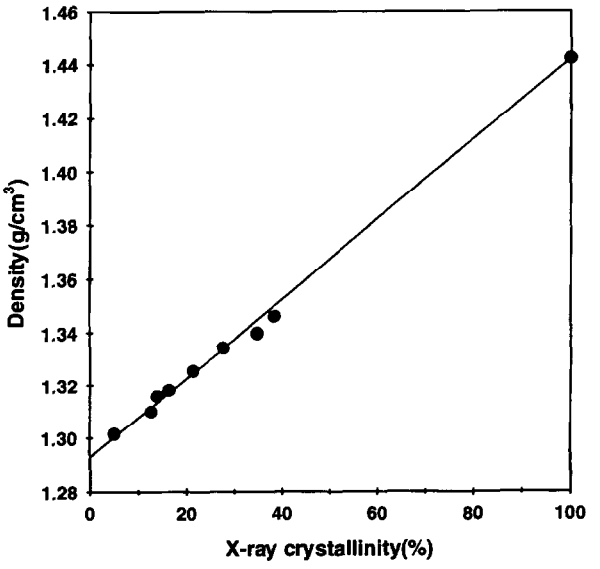

Fig. 4. Relationship between the fiber density and crystallinity measured using WAXD experiments

a wide range of crystallinity depending on the draw ratio. In Fig. 4, extrapolating this relationship to both 100% and zero crystallinity should yield both the crystallographic and amorphous densities and they are 1.442 g cm^{-3} for 100% crystallinity and 1.293 g cm^{-3} for 0% crystallinity (amorphous density), respectively. This extrapolated crystallographic density is in excellent agreement with that calculated from the unit cell parameters. The density difference between totally amorphous and 100% crystalline state is about 0.15 g cm^{-3}. As a result, as-spun ODPA–DMB fibers show about 5% crystallinity while highly drawn fibers with a draw ratio of 4.4 possess about 38% crystallinity.

The overall orientation for the ODPA–DMB fibers of various draw ratios has been measured via optical birefringence experiments and the results are shown in Fig. 5. The birefringence increases gradually with draw ratio but this increase slows down slightly at high draw ratios. In the triclinic lattice, in principle, spots near the meridian can be used to determine the crystal orientation if they are well separated. In the highly drawn ODPA–DMB WAXD fiber pattern (Fig. 1) three reflection spots near the meridian can be found. However, they are not isolated enough to provide a clear determination of crystal orientation. Furthermore, their intensities are not strong enough to generate a good signal–noise ratio. The intensity of the 001 reflection, which is on the first layer, is also not strong enough to provide clear information about the degree of crystal orientation. However, the intensity of the first spot on the equatorial direction, which turned out to be the 110 reflection, is very strong and isolated. It has thus been used to determine the crystal orientation although the direction of 110 reflection is not the

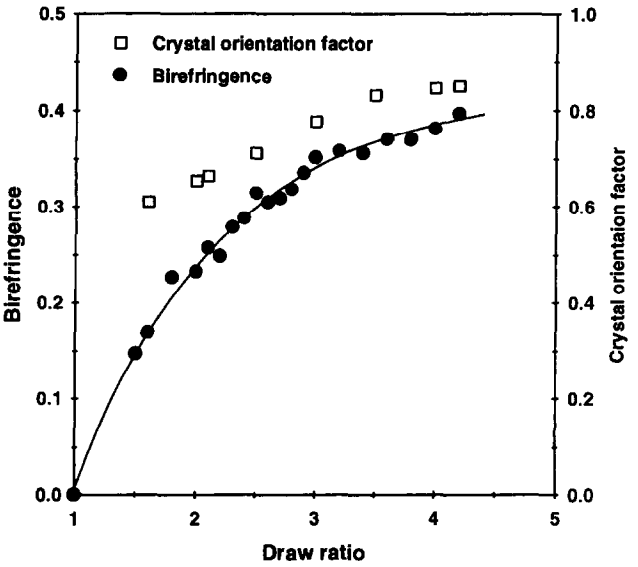

Fig. 5. Degrees of overall orientation and crystal orientation with respect to draw ratio.

same as the fiber direction, being more or less perpendicular to the chain molecular direction.

The degree of crystal orientation at different draw ratios calculated from Hermans equation (Eq. (1)) is also included in Fig. 5. Although it also increases with draw ratio, the degree of crystal orientation builds up relatively fast during the initial stage of the drawing process compared to the degree of overall orientation (Fig. 5). For example, at a draw ratio of 2.0 the degree of crystal orientation of the ODPA–DMB fibers is about 0.65 while it becomes 0.83 at a draw ratio of 3.5. At a draw ratio of 4.0, this degree of orientation reaches 0.85. Further increase in draw ratio does not produce significant improvement in the degree of crystal orientation. The change in the increase of crystal orientation occurs at a draw ratio of about 3–3.5, at which the increasing tendency of crystallinity and density also changes. However, the degree of overall orientation continues to increase at high draw ratio. Since the crystal orientation reaches almost the same value above a draw ratio of 4, it can be expected that the main contribution to the degree of overall orientation in the high draw ratio is attributed to the non-crystalline regions of the fibers. Similar observations have been reported for the other synthetic fibers such as polyesters, polyamides [13–15] and polyimides [3,4].

3.3. *Mechanical tensile properties*

Fig. 6 shows a series of tensile stress–strain curves at room temperature for ODPA–DMB single filaments at different draw ratios. As the draw ratio increases, the strain at

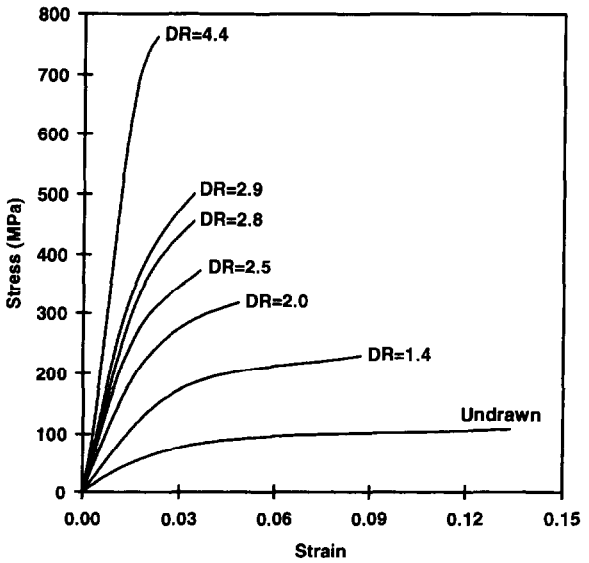

Fig. 6. Set of stress–strain curves of ODPA–DMB fibers at different draw ratios.

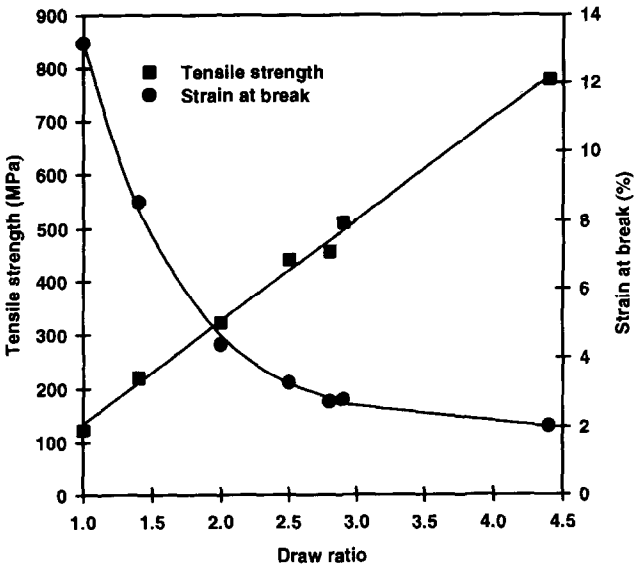

Fig. 7. Tensile strength and strain at break changes with draw ratios.

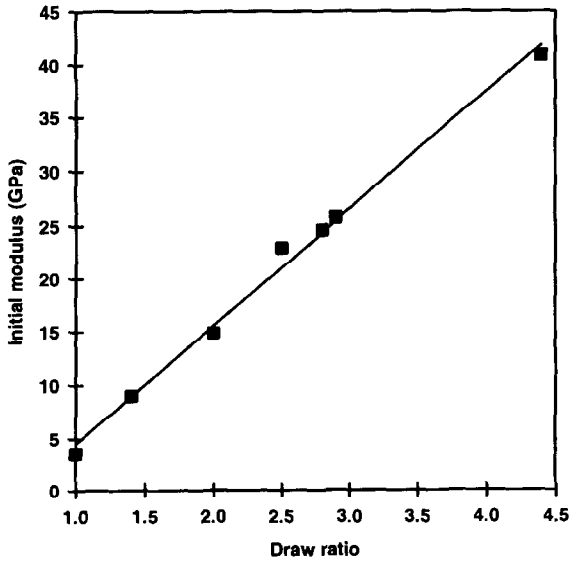

Fig. 8. Tensile modulus change with draw ratios.

break considerably decreases while the corresponding tensile stress and modulus increase. Figs. 7 and 8 show the quantitative changes of the tensile strength and modulus with respect to draw ratio in ODPA–DMB fibers, respectively. Almost linear relationships of both tensile strength and modulus changing with draw ratio can be found. The tensile strength is 123 MPa, having a strain of 13% for as-spun OPDA–DMB fibers, and it changes to 770 MPa with 2.1% strain for fibers having a draw ratio of 4.4. The corresponding change of the modulus (the initial slope of the stress–strain curves in Fig. 6) for the as-spun fiber of 3.7 GPa to 41 GPa for the fiber with a draw ratio 4.4 can also be observed. The modulus of the fiber increases over ten times when it was drawn 4.4 times the original length.

Generally speaking, the increase in the modulus can be explained by the enhancement of crystalline and non-crystalline orientation and degree of crystallinity in the fiber with increasing draw ratio. From Figs. 7 and 8, the tensile properties are increased almost linearly even at higher draw ratios. The increase in the crystallinity and degree of crystal orientation (Figs. 3–5) levels off at high draw ratios. The increase of tensile properties observed in Figs. 6–8 must thus be due partially to the increase of orientation in the non-crystalline regions of the ODPA–DMB fibers.

It is also interesting to observe that the draw ratio is critically dependent upon the pre-existing structure in as-spun fibers developed during the fiber spinning. When the fiber was spun at a relatively high take-up speed, chain molecules more or less aligned which leads to certain degree of orientation. In the drawing process at elevated temperature, the fiber can only be elongated to a relatively low draw ratio. For example, less than 20% of overall orientation and 10% crystallinity presented in the as-spun fibers drastically affect the drawability and the maximum draw ratio of the fiber (only up to about 3). On the other hand, fibers spun using a very slow take-up speed can maximize the draw ratio up to around 5. This structure influence is attributed to the crystallization process taking place during the drawing. The fibers with some degree of orientation and crystallinity are easily further crystallized during the drawing process. The formation of crystals in the fibers, without achieving full orientation, hampers the chain molecular mobility and, therefore, the orientation process. As a result, maximum draw ratio and high tensile properties cannot be obtained. The as-spun fibers without pre-existing structure quickly align themselves above the glass transition temperature during drawing at elevated temperatures, and a maximum degree of orientation can be obtained before the massive crystallization takes place. The draw ratio and tensile properties thus reach high values.

4. Conclusion

We have reported on new aromatic polyimide fibers spun from pre-formed ODPA–DMB polyimide solution. The crystal unit cell symmetry and dimensions have been determined as triclinic having $a = 1.05$ nm, $b = 0.871$ nm, $c = 2.14$ nm, $\alpha = 45.6°$, $\beta = 53.7°$ and $\gamma = 61.4°$. Although the crystallinity and degree of orientation increase with draw ratio, the overall and crystal orientation develop differently in the high draw ratio region. The improvement of the tensile properties in this draw ratio is attributed

to the increase of orientation in the non-crystalline region of the fibers. The pre-existing structure in the fiber introduced during the fiber spinning drastically affects the draw ratio and final mechanical properties.

Acknowledgments

YHK acknowledges support from the Yonam Foundation, Korea. This work was supported by SZDC's NSF Presidential Young Investigator Award (DMR-9157738) and The NSF/EPIC Center of Molecular and Microstructure Composites at The University of Akron and Case Western Reserve University.

References

[1] S.Z.D. Cheng, Z.Q. Wu, M. Eashoo, S.L.-C. Hsu and F.W. Harris, Polymer, 32 (1991) 1803.
[2] M. Eashoo, D.X. Shen, Z.Q. Wu, C.J. Lee and F.W. Harris, Polymer, 33 (1993) 3209.
[3] M. Eashoo, Z.Q. Wu, A.Q. Zhang, D.X. Shen, C. Tse, F.W. Harris, S.Z.D. Cheng, B.S. Hsiao and K.H. Gardner, Macromol. Chem. Phys., 195 (1994) 2207.
[4] D.X. Shen, Z.Q. Wu, J. Liu, L.X. Wang, S.K. Lee, F.W. Harris and S.Z.D. Cheng, Polym. Polym. Compos., 2 (1994) 149.
[5] S.Z.D. Cheng and F.W. Harris, Polyimide fibers, Aromatic, in S. Lee (ed.), International Encyclopedia of Polymer Composite, VCH Publishers, N.Y., Vol. 6, 1991, pp. 293–309.
[6] F.W. Harris, in D. Wilson, H.D. Stenzenberger and P.M. Hergenrother (Eds.), Polyimides, Chapman and Hall, New York, 1989, Chapt. 1, pp. 1–37.
[7] S.L.-C. Hsu and F.W. Harris, High-Performance Polym., 1 (1989) 1.
[8] H.H. Yang, Aromatic High-Strength Fibers, Wiley, New York, 1989.
[9] Y.H. Kim, B.S. Moon, F.W. Harris and S.Z.D. Cheng, J. Therm. Anal., in press.
[10] A.A. Hamza and N.I. El-Kader, Textile Res. J., 53 (1983) 205.
[11] M.I. Bessonov, M.M. Koton, V.V. Kudryavtsev and V.V. Lains, Polyimides, Thermally Stable Polymers, Consult. Bureau, New York, 1987.
[12] Z.-Q. Wu, A.-Q. Zhang, D.X. Shen, F. W. Harris and S.Z.D. Cheng, J. Therm. Anal., in press.
[13] E. Balcerzyk, W. Kozkowski, E. Wesol'owska and W. Lemiszkiewicz, J. Appl. Polym. Sci., 26 (1981) 2573.
[14] S.D. Long and I.M. Ward, J. Appl. Polym. Sci., 42 (1991) 1911.
[15] P.B. Rim and C.J. Nelson, J. Appl. Polym. Sci., 42 (1991) 1807.